



HAL
open science

Evidence of two sensitization processes of Nd³⁺ ions in Nd-doped SiO_x films

Chuan-Hui Liang, Julien Cardin, Christophe Labbé, Fabrice Gourbilleau

► **To cite this version:**

Chuan-Hui Liang, Julien Cardin, Christophe Labbé, Fabrice Gourbilleau. Evidence of two sensitization processes of Nd³⁺ ions in Nd-doped SiO_x films. *Journal of Applied Physics*, 2013, 114, pp.033103. 10.1063/1.4813610 . hal-01138698

HAL Id: hal-01138698

<https://hal.science/hal-01138698v1>

Submitted on 2 Apr 2015

HAL is a multi-disciplinary open access archive for the deposit and dissemination of scientific research documents, whether they are published or not. The documents may come from teaching and research institutions in France or abroad, or from public or private research centers.

L'archive ouverte pluridisciplinaire **HAL**, est destinée au dépôt et à la diffusion de documents scientifiques de niveau recherche, publiés ou non, émanant des établissements d'enseignement et de recherche français ou étrangers, des laboratoires publics ou privés.

Evidence of two sensitization processes of Nd³⁺ ions in Nd-doped SiO_x films

C.-H. Liang, J. Cardin, C. Labbé, and F. Gourbilleau

Citation: *Journal of Applied Physics* **114**, 033103 (2013); doi: 10.1063/1.4813610

View online: <http://dx.doi.org/10.1063/1.4813610>

View Table of Contents: <http://scitation.aip.org/content/aip/journal/jap/114/3?ver=pdfcov>

Published by the [AIP Publishing](#)

Articles you may be interested in

[Direct and indirect excitation of Nd³⁺ ions sensitized by Si nanocrystals embedded in a SiO₂ thin film](#)

J. Appl. Phys. **110**, 113518 (2011); 10.1063/1.3667286

[Effect of annealing and Nd concentration on the photoluminescence of Nd³⁺ ions coupled with silicon nanoparticles](#)

J. Appl. Phys. **108**, 113114 (2010); 10.1063/1.3510521

[Nd-doped GdVO₄ films prepared by pulsed-laser deposition on SiO₂/Si substrate](#)

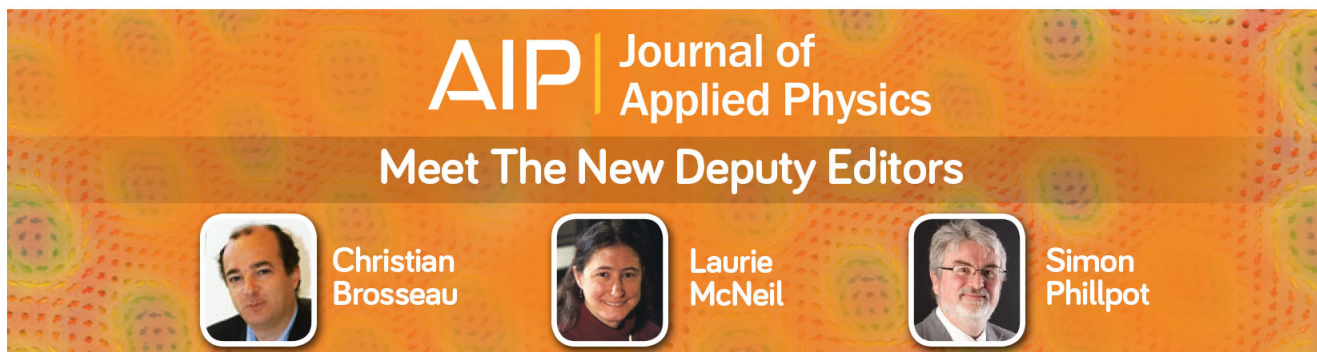
Appl. Phys. Lett. **86**, 151908 (2005); 10.1063/1.1898439

[Spectroscopic study of Nd-doped amorphous SiN films](#)

J. Appl. Phys. **96**, 1068 (2004); 10.1063/1.1760843


[The Nd-nanocluster coupling strength and its effect in excitation/de-excitation of Nd³⁺ luminescence in Nd-doped silicon-rich silicon oxide](#)

Appl. Phys. Lett. **83**, 2778 (2003); 10.1063/1.1615837



AIP | Journal of Applied Physics

Meet The New Deputy Editors

	Christian Brosseau		Laurie McNeil		Simon Phillpot
---	---------------------------	---	----------------------	---	-----------------------

Evidence of two sensitization processes of Nd³⁺ ions in Nd-doped SiO_x films

C.-H. Liang,^{a)} J. Cardin, C. Labbé, and F. Gourbilleau^{b)}

CIMAP, UMR CNRS/CEA/ENSICAEN/UCBN, Ensicaen, 6 Bd Mal Juin, 14050 Caen Cedex 4, France

(Received 14 March 2013; accepted 25 June 2013; published online 16 July 2013)

This paper aims to study the excitation mechanism of Nd³⁺ ions in Nd-SiO_x ($x < 2$) films. The films were deposited by magnetron co-sputtering followed by a rapid thermal annealing at temperature T_A ranging from 600 to 1200 °C. Two different photoluminescence (PL) behaviors have been evidenced in SiO_x layers depending on the annealing temperature. For low T_A ($T_A < 1000$ °C), the recorded visible PL originates from defects energy levels while for high T_A ($T_A > 1000$ °C), the visible emission emanates from recombination of excitons in Si nanoclusters. When doped with Nd³⁺ ions, the visible PL behaviors of Nd-SiO_x films follow the same trends. Nd³⁺ PL was investigated and its decay rate was analyzed in detail. Depending on the annealing conditions, two types of sensitizers have been evidenced. Finally, maximum Nd³⁺ PL emission has been achieved at around 750 °C when the number of Nd³⁺ ions excited by the two types of sensitizers reaches a maximum.

© 2013 AIP Publishing LLC. [<http://dx.doi.org/10.1063/1.4813610>]

I. INTRODUCTION

As a leading semiconductor material in the microelectronic industry, silicon has received significant attention on its optical functionality in these last years aiming at integrating photonics with semiconductor microelectronics.^{1,2} However, suffering from the indirect nature of its band gap, bulk Si shows poor emission efficiency. Fortunately, two important results have been achieved by decreasing the Si grain size to the nanoscale range. On one hand, the nature of Si band gap changes from indirect to quasi-direct with the decrease in grain size.³ This quasi-direct band gap allows room temperature photoluminescence (PL) of Si nanoclusters (Si-ncs) without any phonon assistance. This emission is ranging in the visible spectra from 700 to 900 nm depending on the Si-ncs size.³⁻⁶ On the other hand, Si-ncs can play the role of sensitizer towards rare earth (RE) ions such as Er³⁺ ion⁷⁻¹² or Nd³⁺ ion.¹³ Hence, the effective excitation cross section of RE ions is enhanced by several orders of magnitude and broadened spectrally in the visible range.^{14,15} This result provides the possibility to manufacture less-cost and miniaturized Si-based optoelectronic devices.

To better understand the limiting factors for achievement of such optoelectronic devices, huge effort has been focused on the mechanism of energy transfer from Si-ncs towards Er³⁺ ions. It appears that the Si-ncs:Er³⁺ interaction distance should be less than 2 nm¹⁶ for an effective coupling whose efficiency decreases exponentially with the increasing of distance.¹⁰ Fujii *et al.*¹⁷ observe the coexistence of two processes for Si-ncs:Er³⁺ energy transfer depending on the sizes of the sensitizers. A fast process is attributed due to the large Si-ncs sensitizer, while a slow one is found to depend on the recombination rate of excitons in small Si-ncs. In contrast, Savchyn *et al.*¹² demonstrate the existence of two excitation processes for Er³⁺ ⁴I_{13/2} level involving multi-levels sensitization: fast direct excitation by Si-excess-related

luminescence centers and slow excitation related to the fast excitation of Er³⁺ ions up to the higher energy levels such as ⁴F_{9/2} and ⁴I_{9/2} with subsequent slow relaxation to the ⁴I_{13/2} level. These works agree the origin of Er³⁺ excitation from recombination of generated excitons within Si-ncs and subsequent energy transfer to the nearby Er³⁺ ions. Even though a great number of papers have been published on the Si-based matrices co-doped with Er³⁺ and Si-ncs, evidence of the achievement of net gain from such a system has been presented in only one report.¹⁸ This is due to the nature of the three-level electronic 4f structure for the Er³⁺ ions leading to a threshold power necessary to get population inversion and to the possibility of reabsorption of photon emitted by the neighboring Er³⁺ ions. In contrast, the Nd³⁺ ions emitting in four-level configuration (1.06 μm) do not have a threshold pump power for inverting population and there is no reabsorption of the emitted light at 1.06 μm. Moreover, the up-conversion is negligible with Nd³⁺ ions¹⁹ emitting at 1.06 μm compared to Er³⁺ ions²⁰ emitting at 1.53 μm. Consequently, net gain should be achievable with Nd³⁺ ions in easier way than with Er³⁺ ions.

However, the study on excitation mechanism of Nd³⁺ ions in Nd-SiO_x films is still rather rare by comparison to its Er³⁺ ions counterpart. After the discovery of energy transfer from Si-ncs to Nd³⁺ ions,²¹ several groups²²⁻²⁴ investigated the energy transfer with the goal of improving the Nd³⁺ emission properties. Our previous work²⁴ evidences that high Nd³⁺ content incorporated into the layers would form Nd₂O₃ clusters leading to the quenching of the Nd³⁺ PL. Moreover, Watanabe *et al.*²⁵ point out that the Si-ncs size plays an important role in the Si-ncs:Nd coupling. The authors show that the Si-ncs:Nd energy transfer is more effective with smaller Si-ncs. This is explained by a good match of energy band gap in small Si-ncs with Nd³⁺ excited energy levels (higher than ³F_{3/2}). Therefore, the discussion on excitation mechanism of Nd³⁺ ions should include an investigation of Si-ncs PL properties. Two main models on the origin of Si-ncs emission have been proposed on the basis of both experimental and theoretical studies. The first

^{a)}Electronic mail: chuan-hui.liang@ensicaen.fr

^{b)}Electronic mail: fabrice.gourbilleau@ensicaen.fr

model depicts the quantum confinement effect,²⁶ which in general explains the evolution of Si-ncs PL versus its size depending on the Si excess and/or annealing treatment.²⁷ The second model considers that the Si-ncs PL is correlated to the presence of defects at the interface between Si-ncs and SiO₂ matrix in SiO_x layers,^{28,29} supporting the PL peak position size-independent.³⁰

In this paper, we investigate the optical properties of SiO_x and Nd-SiO_x films annealed using rapid thermal annealing (RTA) process. The influence of Si-ncs PL origins on the excitation mechanism of Nd³⁺ ions is investigated depending on the annealing conditions.

II. EXPERIMENT

Undoped- and Nd-doped-SiO_x ($x < 2$) films of about 350 nm thick were deposited by magnetron co-sputtering of two (SiO_x) or three (Nd-SiO_x) confocal cathodes under a plasma of pure argon. The p-type monocrystalline Si or fused silica substrates were used and maintained at 500 °C during the growth. The plasma power density for Nd₂O₃, Si, and SiO₂ targets were fixed at 0.30, 1.48, and 8.88 W/cm², respectively. After deposition, the films were submitted to RTA process under N₂ for variable durations, t_A , and different temperatures, T_A , ranging from 1 min to 1 h and 600 to 1200 °C, respectively. The microstructural characteristics were obtained by RAMAN and Fourier transform infrared (FTIR) spectroscopies. The optical properties were achieved by means of PL experiments. These latter were carried out using the 488-nm-line of a CW Ar⁺ laser (Innova 90C Coherent), which is a non-resonant wavelength for Nd³⁺ ions.³¹ PL decay times have been recorded at the maximum PL intensity for Si-ncs peak and 920 nm for Nd³⁺ ions after short excitation pulses (5 ns) at full width at half maximum of a tunable pulsed laser (EKSPLA NT 340 OPO pumped by a YAG:Nd laser) set at 488 nm with a repetition rate of 10 Hz. The focusing beam was 500 μm with an average energy of 15 mJ. The PL decay was recorded with an appropriated electronic and detector (PM R5509-73 Hamamatsu) on a digital oscilloscope (Tiektronix tds 3012).

III. RESULTS AND DISCUSSION

The two kinds of films, SiO_x and Nd-SiO_x, object of the present study, have the same value of O/Si ratio ($x = 1.74$). The x value was calculated as shown in our previous paper³² using the equation

$$x = 0.02\nu - 19.3, \quad (1)$$

where ν is the transverse optical (TO₃) peak position in FTIR spectrum collected at normal incidence. As a consequence, the Si excess (Si_{ex}) is found to be 4.7 at. % using the following relation:

$$Si_{ex}(at\%) = [(2 - x)/(2 + 2x)]100. \quad (2)$$

This silicon excess value has been confirmed by Rutherford backscattering experiments, which have given a Nd content of about 5×10^{19} Nd cm⁻³.

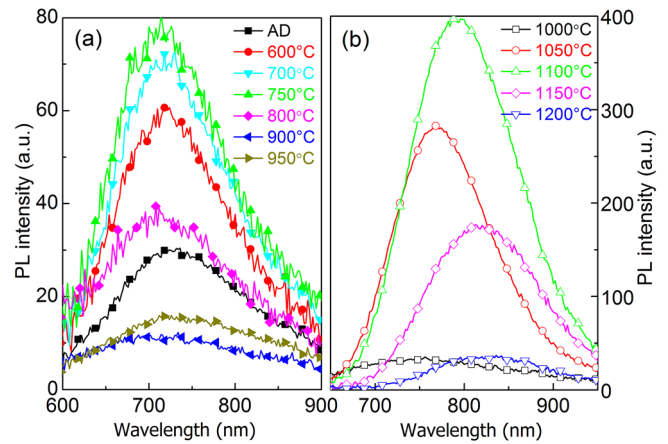


FIG. 1. The PL spectra of SiO_x films annealed at the indicative temperature with 1 min duration. The left (a) corresponds to T_A lower than 1000 °C while the right (b) to high T_A higher than 1000 °C. AD is the abbreviation of as-deposited.

A. Photoluminescence properties of SiO_x films

The PL properties of SiO_x films were investigated as a function of T_A . The spectra are separately shown in Figure 1(a) for low T_A less than 1000 °C and Figure 1(b) for high T_A more than 1000 °C. As noticed on these two graphs, the emission bands peak at different wavelengths depending on the T_A range. Thus, the emission peaks obtained for low T_A will be defined as E_L ; while for high T_A , the recorded emission peaks will be called E_H . To easily catch the evolution trend, both integrated peak intensity and maximum peak position have been determined and are presented in Figure 2. The E_L peak intensity first increases to reach a maximum for $T_A = 750$ °C before decreasing for higher annealing temperatures. This could be explained by a passivation of some non-radiative centers with increasing T_A up to 750 °C and for T_A above 750 °C by a decrease of the number of emitting centers at the origin of the E_L peak emission. Its position does not change with T_A peaking at around 720 nm. The exact origin of this E_L peak is still unclear. Wang *et al.*³⁰ and Wora Adeola *et al.*³³ have separately observed the very similar E_L peak in their samples. The former attribute it to surface states while the latter to band tails states. Therefore, at this level of discussion, we ascribe this E_L peak to defects related radiative states which origin will be specified later in this paper. Comparatively for T_A higher than 1000 °C, the E_H peak

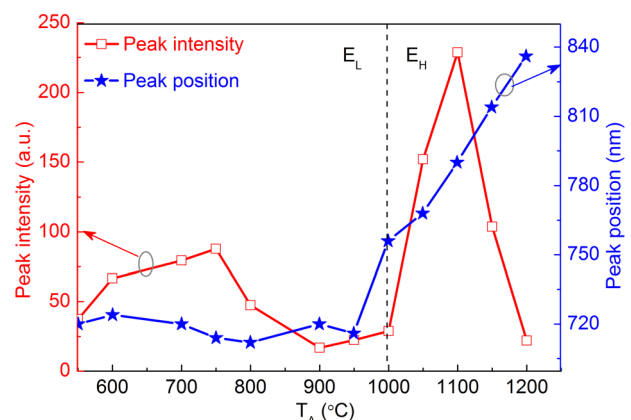


FIG. 2. Peak intensity (left scale) and position (right scale) of SiO_x films versus T_A .

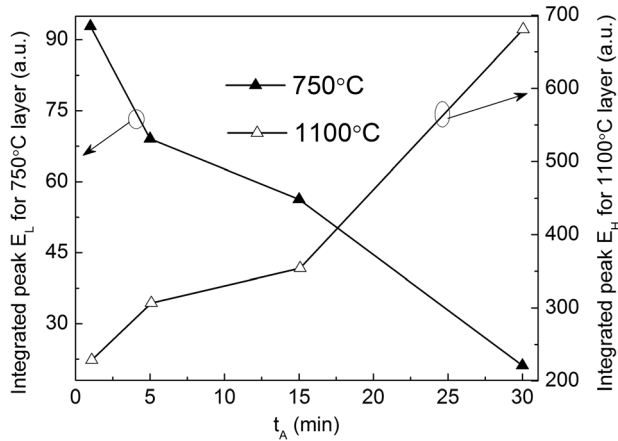


FIG. 3. E_L and E_H peak intensity versus t_A for SiO_x films annealed at 750°C (left scale) and 1100°C (right scale), respectively.

intensity rises up abruptly till a maximum at $T_A = 1100^\circ\text{C}$ and thereafter drops down to a very low value for the highest annealing temperature ($T_A = 1200^\circ\text{C}$). However, the maximum E_H intensity is more than three times higher than the one achieved for E_L peak after annealing at $T_A = 750^\circ\text{C}$. The band positions red-shift from 756 to 836 nm with increasing T_A , allowing of attributing the E_H peak to the quantum-confined excitonic states in Si-ncs.²⁶ This evolution of E_H intensity versus T_A is related both to the passivation of non-radiative channels and the Si-ncs density increase up to 1100°C. If the former continues for higher annealing temperature, the latter will decrease due to a Si-ncs size growth over the quantum confinement limit. Such an oversize growth explains the quench of the PL observed for temperature as high as 1200°C. Note that both E_L and E_H peaks are related to the Si excess incorporated in the SiO_2 matrix as no emission was observed from pure SiO_2 sputtered films annealed at any T_A .

To further analyze the different PL behaviors between low- and high- T_A layers, two typical annealing temperatures (750 and 1100°C) corresponding to the maximum PL intensities achieved were set to study the effect of annealing time t_A . The evolutions of peak intensity as a function of t_A are presented in Figure 3. It can be noticed that the E_L peak intensity gradually decreases with time for the 750°C-annealed samples while E_H peak significantly increases for the 1100°C-ones, for the same range of time. This PL evolution is another evidence of different excitation-de-excitation mechanisms: radiative defects controlled at 750°C while quantum confinement controlled at 1100°C. When the annealing duration is increased, the radiative defects are quenched at 750°C probably due to the rearrangement of Si and/or O atoms, while the 1100°C-extended annealing could mainly passivate the non-radiative defects such as stressed bond angles, distorted bond length in host. In high temperature range, Garrido Fernandez *et al.*³⁴ have obtained the same PL behavior versus t_A . They observe that during annealing process the nucleation and growth of Si-ncs are almost completed in a few minutes and the average Si-ncs diameter remains constant for longer annealing times. Thus, increasing annealing time up to 30 min favors achievement of high Si-ncs density but remains sufficiently short to avoid the growth

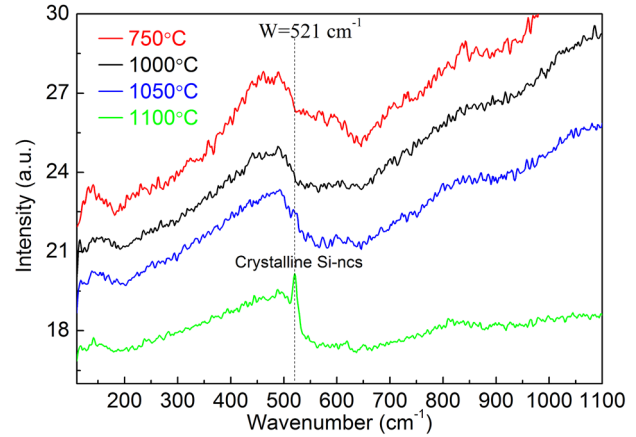


FIG. 4. RAMAN spectra of the SiO_x films deposited on quartz substrate and annealed at indicated T_A for 1 min.

of large Si-ncs, which are detrimental for the quantum confinement process.³⁵ Moreover, such extra annealing time favors the recovering of the non-radiative channels.

B. Microstructural characterization

To understand the above PL properties, the evolution of film microstructure versus T_A has been analyzed by means of RAMAN spectroscopy (Figure 4). Each curve has a broad band peaking at $\sim 480 \text{ cm}^{-1}$ attributed to amorphous Si agglomerates. Such a result is in agreement with previous work showing that the formation of amorphous Si agglomerates in similar thin films starts to occur at about 600°C.³⁶ By increasing T_A up to 1100°C, a sharp peak at around 521 cm^{-1} assigned to crystalline Si-ncs appears while, in the same time, the 480 cm^{-1} -band intensity decreases. This convincingly certifies that the $T_A = 1100^\circ\text{C}$ annealing promotes the formation of Si nanocrystals. The results of RAMAN experiments on the Nd-doped SiO_x thin films (not shown here) follow the same trends as results obtained on undoped films. This is supported by the fact that the low Nd content incorporated may not affect the formation of either amorphous or crystalline Si-ncs.

Figure 5 shows the evolution of FTIR spectra for SiO_x films annealed at different temperatures. There are two main

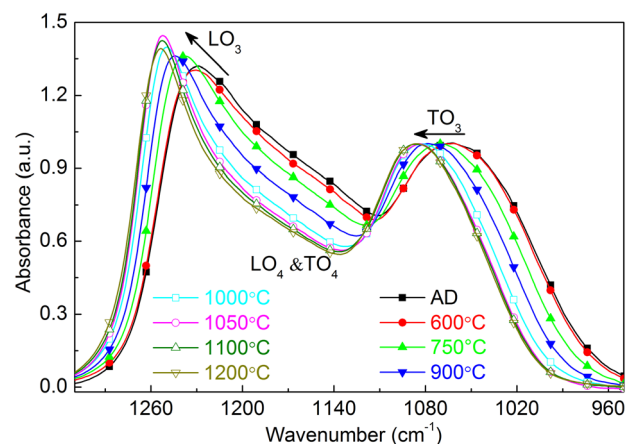


FIG. 5. FTIR spectra recorded at Brewster angle of 65° for SiO_x films deposited on a Si wafer and annealed at indicated T_A during 1 min. The spectra were normalized with respect to the TO_3 band intensity.

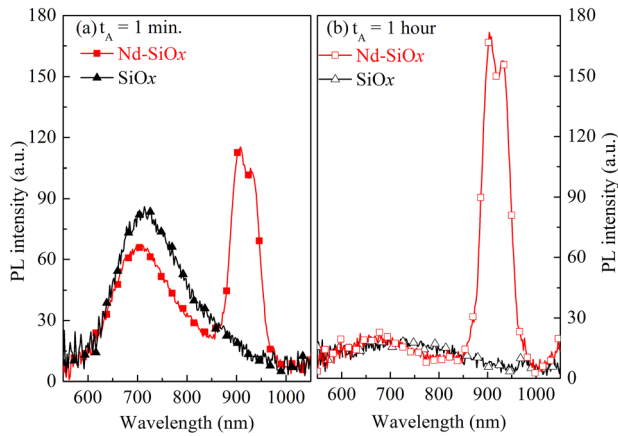


FIG. 6. PL spectra of Nd-SiO_x and SiO_x films annealed at 750 °C during (a) 1 min and (b) 1 h.

bands attributed to longitudinal optical (LO₃) and TO₃ phonons of Si-O bonds. The relative intensity of the former peaking in the 1230–1255 cm⁻¹ range increases with T_A up to 1050 °C, and then slightly decreases for higher T_A. According to the work of Olsen and Shimura,³⁷ LO₃ band intensity corresponds to the number of Si-O-Si bonds at 180° present at the Si/SiO₂ interface. Consequently, this is the signature of the increasing formation of Si-ncs in our film upon annealing temperature up to 1050 °C. The continuously increase of T_A will then favor the growth of Si-ncs size leading to the decrease of the Si-ncs density and thus the number of Si-O-Si bonds at the Si/SiO₂ interface. As a consequence, a slight decrease of the LO₃ mode intensity is noticed. Concerning the TO₃ mode, it blue-shifts from 1052 to about 1081 cm⁻¹ with increasing T_A. This progressive shift towards the stoichiometric position of amorphous SiO₂ (1081 cm⁻¹) is indicative of the phase separation between Si and SiO₂ occurring in the film. This is confirmed by the decrease of the disorder in the matrix as evidenced by the evolution of the intensity of the LO₄ and TO₄ pair modes with T_A.

C. Comparison of Nd-SiO_x PL properties with SiO_x films

To study the excitation mechanism of Nd³⁺ ions in Nd-SiO_x system, the PL experiments are performed on Nd-doped SiO_x layers annealed at 750 and 1100 °C which correspond to the two temperatures allowing achievement of the maximum intensity for E_L and E_H peaks, respectively. Figure 6(a) shows the PL spectra of Nd-SiO_x and SiO_x films annealed at 750 °C during 1 min. The significant Nd³⁺ PL peak from the de-excitation from the ⁴F_{3/2} to ⁴I_{9/2} level at around 920 nm is observed for Nd-doped layer excited with the non-resonant 488 nm-Ar laser wavelength. This implies the existence of Nd³⁺ sensitizers present in the SiO_x matrix. The occurrence of an energy transfer from sensitizers to Nd³⁺ ions is evidenced by the concomitant lowering E_L peak intensity compared to that from undoped SiO_x layer.

To confirm this behavior, investigation of the visible and Nd³⁺ PL intensities as a function of annealing duration has been carried out (Figure 7). One can noticed that the

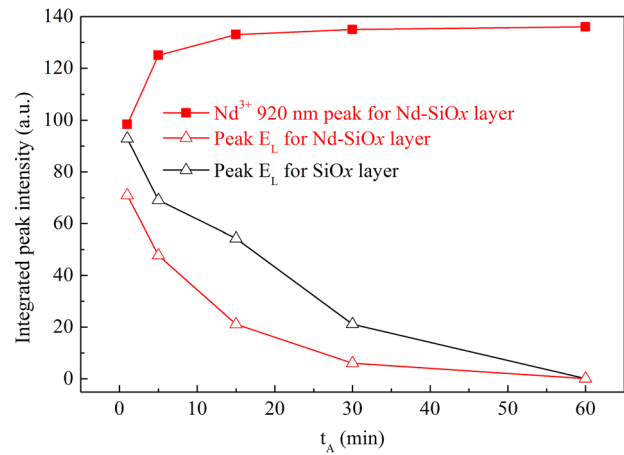


FIG. 7. Integrated peak intensities of Nd-SiO_x and SiO_x films annealed at 750 °C versus t_A.

visible E_L peak intensity decreases versus t_A for both SiO_x and Nd-SiO_x films. As explained above, this evolution can be ascribed to the recovering of the radiative defects. For at least t_A ≤ 30 min, the E_L peak intensity from Nd-doped SiO_x layer annealed at 750 °C shows a lower value than that of undoped one. Such a behavior is an evidence of an efficient energy transfer from these radiative defects to Nd³⁺ ions states, playing the role as Nd³⁺ sensitizers as mentioned above. Concerning the Nd³⁺ emission evolution at 920 nm, it increases until 15 min of annealing and saturates afterward. Such saturation may be attributed to (i) the passivation of some non-radiative defect and/or (ii) the existence of another type of sensitizers. Moreover, we have observed in the Figure 3 a decrease of the low T_A type Nd³⁺ sensitizer (E_L peak) with longer annealing, which should contribute to a decrease of the Nd³⁺ PL intensity. Consequently, those trends of visible and Nd³⁺ PL intensities are a signature of the existence of another type of sensitizers that also excite efficiently the Nd³⁺ ions (Figure 6(b)). As demonstrated in our previous work,³⁸ such sensitizers grown at low T_A contain a few Si atoms (less than 15 atoms) and will be here named atomic scale sensitizers (ASSs). They differ from the luminescence centers proposed by Savchyn *et al.*³⁹ Since using also a RTA of 100 s, they observed always a PL peak position shift, which is in disagreement with our results (seen Figure 1(a)).

When annealed at higher temperature (1100 °C), the intensity of E_H peak falls down by about 8 times after Nd incorporation (Figure 8). It is thus supposed that most of emitters transfer energy to their nearby Nd. One can notice that the position of E_H peak shifts from about 790 to 730 nm after Nd incorporation. This shift is probably explained by the two Nd³⁺ absorption bands peaking at about 750 and 808 nm³¹ and is a confirmation of the energy transfer process involved. Nevertheless, the Nd³⁺ PL intensity achieved at such T_A appears very low. This demonstrates the E_H peak emitters formed at this high temperature act as sensitizer of Nd³⁺ ions, but unfortunately, this efficient energy transfer process suffers from Nd₂O₃ clusters formation and/or a too large sensitizer-Nd³⁺ distance. This can explain that the drop of Si-ncs PL does not lead to a high PL emission of the Nd³⁺

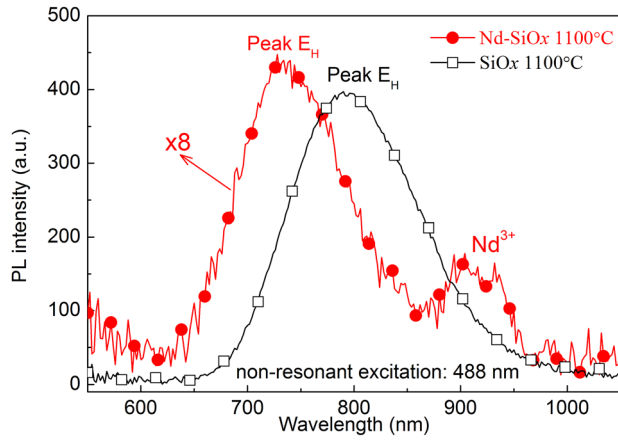


FIG. 8. PL spectra of Nd-SiO_x and SiO_x films annealed for 1 min at 1100 °C.

ions. In addition, the effect of annealing duration was investigated at 1100 °C. The E_H peak intensity of Nd-SiO_x film gradually increases with increasing t_A (data not shown here), presenting thus a similar trend to that achieved for undoped layer (Figure 3).

This paragraph will address the effect of T_A on Nd³⁺ PL properties (Figure 9). Even though the as-deposited layer clearly shows PL, the intensity increases with T_A and is enhanced by a factor 2.5 upon annealing at 750 °C before decreasing for higher T_A . The optimized temperature at 750 °C corresponding to maximum Nd³⁺ PL may be explained by the fact that both matrix ordered degree and coupled Nd³⁺ number evolve in opposite trend with annealing temperature. For the former, the FTIR spectra reported in Figure 5 have evidenced the attenuation of LO₄ and TO₄ pair mode with increasing T_A . Such an evolution implies that the film matrix gradually becomes ordered, which would favor the Nd³⁺ emission by decreasing the non-radiative paths. The concomitant increase of the LO₃ intensity with T_A up to 1050 °C suggests an increase of Si-ncs density also favoring an enhancement of Nd³⁺ emission. For the latter, the visible E_L peak (Figure 1(a)) is quenched with T_A higher than 750 °C attesting the decreasing of radiative defect. When $T_A \geq 750$ °C, the Nd³⁺ ions were consumed by the formation

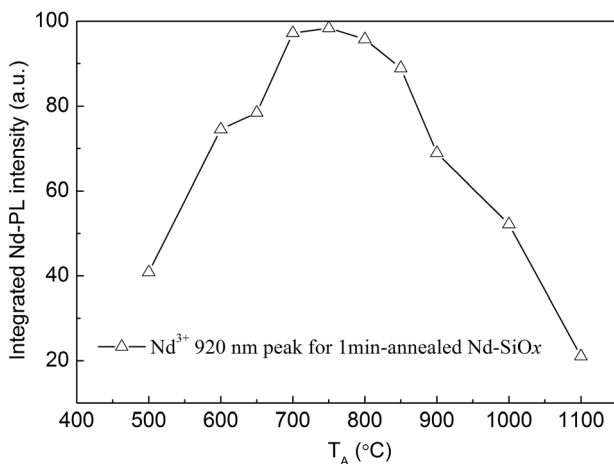


FIG. 9. Evolution of Nd³⁺ PL intensity as a function of T_A for Nd-SiO_x films annealed during 1 min.

of Nd₂O₃ clusters decreasing the coupled Nd³⁺ ions as evidenced by lifetime measurements detailed below. Therefore, a maximum Nd³⁺ PL is reached at the moderated temperature ($T_A=750$ °C). Moreover, it is worth to note that the Nd³⁺ PL at $T_A=900$ °C is still remarkable and only decreases by less than 1.5 times in contrast to that at $T_A=750$ °C. However, the defects emission (E_L peak) almost completely quenches at about 900 °C as shown in Figure 1(a). This again evidences the existence of atomic scale sensitizers apart from the radiative defects.

D. Analysis of both visible PL and Nd³⁺ infrared PL decay curves

Lifetimes τ measured on E_L and E_H peaks do not show a single exponential trend, therefore as a first approach the integrated Eq. (3)⁴⁰ was used in order to fit the decay curve

$$\tau = \int \frac{I}{I_0} dt, \quad (3)$$

where I is a time dependent peak intensity while I_0 is the intensity at $t=0$ s. For E_L peak, the lifetimes of both doped and non-doped films are low and invariable at about 2 μ s as shown in Figure 10. This confirms that the visible E_L peak originates from the defects.⁴¹ For E_H peak from non-doped SiO_x film, the lifetime increases dramatically and holds a value of 29 μ s for 1100 °C-SiO_x film. This value is indicative that E_H peak originates from the exciton recombination confined by quantum effect inside Si-ncs.⁴² In contrast for Nd-SiO_x film annealed at 1100 °C, this lifetime value decreases to 3.6 μ s. This decrease is due to the energy transfer to Nd³⁺ ions as described by the effective lifetime deduced from rate equation⁴³ in the sensitizer:Nd system

$$\tau_{Nd-SiO_x} = \frac{\tau_{SiO_x}}{1 + KN_{Nd}^0 \tau_{SiO_x}}, \quad (4)$$

where τ_{Nd-SiO_x} is the E_L or E_H peak lifetime for Nd-SiO_x film while τ_{SiO_x} corresponds to the non-doped SiO_x film lifetime; K is the coupling constant between sensitizers and

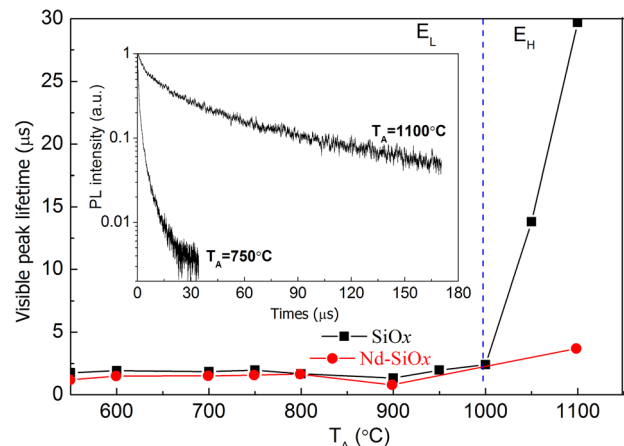


FIG. 10. Evolution of PL lifetimes measured on peak E_L and E_H versus T_A for 1 min-annealed SiO_x and Nd-SiO_x films detected at the maximum point of each peak. The inset shows the PL decay curves for SiO_x films annealed at 750 and 1100 °C.

Nd^{3+} ions; and N_{Nd}^0 is the Nd^{3+} density in the fundamental state. The term $KN_{\text{Nd}}^0\tau_{\text{SiO}_x}$ describes phenomenologically⁴⁴ the coupling between sensitizers and Nd^{3+} ions. Therefore, the decrease of $\tau_{\text{Nd-SiO}_x}$ with respect to τ_{SiO_x} can be ascribed to the increasing of the coupling term $KN_{\text{Nd}}^0\tau_{\text{SiO}_x}$ and thus evidence the energy transfer to Nd^{3+} ions. In Nd-SiO_x films annealed at $T_A < 1000^\circ\text{C}$, the lifetime $\tau_{\text{Nd-SiO}_x}$ is slightly lower than τ_{SiO_x} , taking into account our experimental uncertainties. For layers annealed at $T_A > 1000^\circ\text{C}$, the lifetime $\tau_{\text{Nd-SiO}_x}$ is 10 to 20 times lower than SiO_x lifetime (Figure 10). Consequently, for low T_A , Nd-SiO_x layers have a weaker coupling term $KN_{\text{Nd}}^0\tau_{\text{SiO}_x}$ compared to higher one. The efficiency η of energy transfer can be estimated by the following equation:⁴⁵

$$\eta = 1 - \frac{\tau_{\text{Nd-SiO}_x}}{\tau_{\text{SiO}_x}}. \quad (5)$$

One can obtain that in Nd-SiO_x films annealed at $T_A < 1000^\circ\text{C}$, the efficiency is lower than 10%, while η reaches about 90% for 1100°C -annealed layer. Notwithstanding, the weaker sensitizer: Nd coupling regime and lower efficiency for the low T_A , the highest PL intensity is achieved. Such a feature can be explained by the larger number of sensitized Nd^{3+} ions due to the larger density of both radiative defects and atomic scale sensitizers (low T_A) than that of Si-ncs sensitizers (high T_A).

The decay rate of Nd^{3+} infrared PL at 920 nm has a non-exponential nature as seen from the Figure 11 inset (a). For all the films, the Nd^{3+} PL decay rate was fitted by a two-exponential decay model

$$I(t) = A_1 \exp\left(-\frac{t}{\tau_1}\right) + A_2 \exp\left(-\frac{t}{\tau_2}\right). \quad (6)$$

Fast (τ_1) and slow lifetimes (τ_2) have been reported in Figure 11, and the corresponding component of lifetime ($\frac{A_1}{A_1+A_2}, \frac{A_2}{A_1+A_2}$) is described in the inset (b). On one hand, the fast lifetime is shorter than 24 μs , while the slow one is in

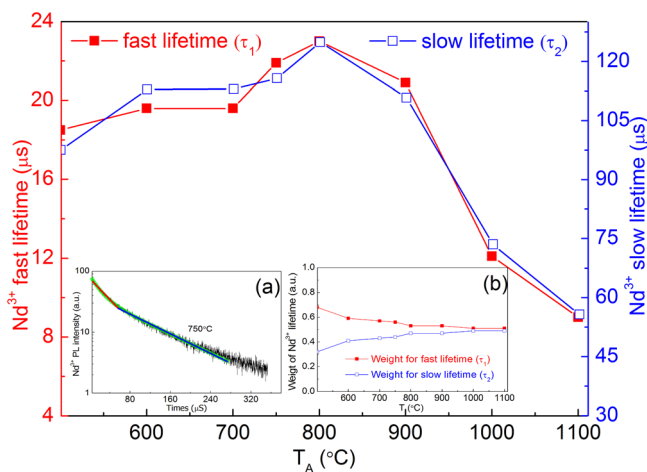


FIG. 11. Evolution of Nd^{3+} PL lifetime at 920 nm versus T_A . The inset (a) is a representative decay rate of 750°C Nd-SiO_x PL, fitted by a two-exponential decay model, while the inset (b) is the component of Nd^{3+} fast or slow lifetime.

the 50–130 μs range. It is observed that both of them gradually increase followed by a dramatic decrease. The maximum is achieved after an annealing at $T_A = 800^\circ\text{C}$. This evolution versus T_A is comparable to the results reported by Li *et al.*⁴⁶ explaining that the local environment of Nd^{3+} ions is deteriorated because of the formation of Nd_2O_3 clusters after annealing at high temperatures. Such a rare earth clusterization has been also observed in a similar sputtered system as demonstrated in our study using atom probe tomography technique.³⁸ On the other hand, the component of fast lifetime decreases from 0.68 to 0.51, in Figure 11 inset (b), while the slow case increases from 0.32 to 0.49. This indicates that (i) the fast lifetime dominates the Nd^{3+} emission for all the layers, and that (ii) the contribution of slow lifetime to Nd^{3+} PL gradually increases with T_A .

E. Energy transfer mechanism

The energy transfer from sensitizers present in SiO_x matrix to Nd^{3+} ions has been demonstrated using a non-resonant excitation as described above and now our purpose is to analyze this transfer process in more details (Figure 12). The absorption spectrum (Figure 12 (ii-b)) of Nd^{3+} ions in Nd -doped SiO_2 film presents four typical absorption bands peaking at about 880, 808, 750, and 585 nm. They correspond to the transitions from the ground level $^4I_{9/2}$ to the excited level $^4F_{3/2}$, $^4F_{5/2}$, $^4F_{7/2}$, and $^2G_{7/2}$, respectively.³¹ Thus, from these quantified energy levels and the positions of E_L and E_H emissions, one can propose a scheme of the transfer mechanism as detailed in Figure 12.

For low T_A -annealed Nd-SiO_x layers, ASSs and radiative defects are present in the matrix. Both efficiently sensitize the Nd^{3+} ions, since the intense Nd^{3+} PL has been observed in both samples annealed at 750°C for 1 min and 1 h (Figure 6). When the radiative defects are recovered with T_A , the atomic scale sensitizers, whose density increases with the temperature, dominate the sensitization of the rare earth ions. As a consequence, in this intermediate

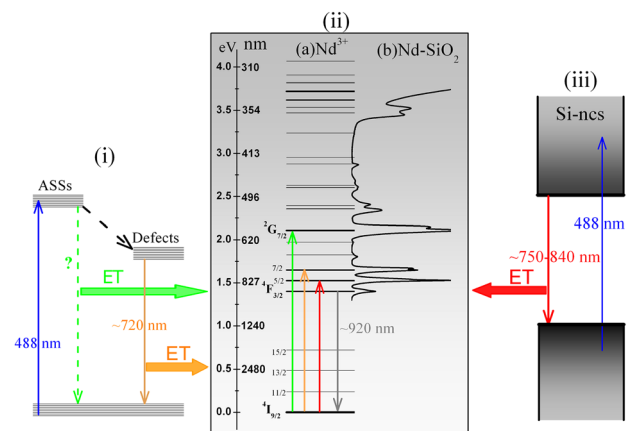


FIG. 12. Schematic illustrations of the Nd^{3+} ions excitation. (i) Energy diagrams of ASSs and defects within the films annealed at $T_A < 1000^\circ\text{C}$, (ii) (a) energy diagram of Nd^{3+} ions and (b) absorption spectrum of Nd^{3+} ions doped in SiO_2 film, and (iii) energy diagram of Si-ncs within the films annealed at $T_A > 1000^\circ\text{C}$. ET is the abbreviation of energy transfer.

temperature range, two paths of sensitization of Nd^{3+} ions will coexist and are at the origin of the radiative recombination from the ${}^4\text{F}_{3/2}$ to the ground state ${}^4\text{I}_{9/2}$ level with an emission at about 920 nm.

In the case of high T_A -annealed Nd-SiO_x layers, the formed Si-ncs have a smaller band gap than in the case of atomic scale sensitizers. These Si-ncs can also transfer their energy to Nd^{3+} ions as demonstrated by the decreasing of Si-ncs PL intensity (Figure 8) as well as its lifetime (Figure 10). But the PL intensity of Nd^{3+} ions achieved after such a treatment is low. Such a feature can be attributed to two phenomena: (i) a cross relaxation process among Nd^{3+} ions occurs due to the formation of Nd_2O_3 clusters as witnessed by its lifetimes (Figure 11), (ii) the formation of Si-ncs as already observed in similar sample doped with Er ions⁴⁷ will lead to an increase of the sensitizer:Nd distance.

For all the Nd-SiO_x layers, a Nd^{3+} ions PL decay with a non-exponential nature was observed and fitted using a double exponential decay model leading to the determination of a fast and a slow components. They present an opposite behavior with the annealing temperature (inset (b) in Figure 11): the former decreases while the latter increases. Horak *et al.*⁴⁸ have attributed the shortening of the decay time to a modification of local density of states (LDOS) brought by the Si interface. This is consequently a signature of the distance between rare earth ions and sensitizer. Considering that the annealing temperature favors the phase separation in our layers,³⁵ higher the temperature is, higher the Sensitizer: Nd^{3+} distance. Thus, one can explain the two components of the PL decay to the different environment of Nd^{3+} ions, which is modified by the annealing treatment. This would explain the observed increase of the ratio of slow over fast components of PL decay with temperature.

IV. CONCLUSION

The microstructure and PL properties were investigated as a function of annealing conditions for SiO_x and Nd-SiO_x layers. It has been demonstrated that for the low T_A - ($T_A < 1000^\circ\text{C}$) annealed layers, the visible E_L peak origins from the defects levels, while quantum confinement effect rules the visible E_H peak for the layers annealed at higher temperature. For the Nd^{3+} emission in Nd-SiO_x layers, the former low T_A -layers present high intensity while the latter high T_A -layers have low one. The high PL intensity achieved at 920 nm has been attributed to the high density of sensitizers present in the layers that are able to transfer efficiently their energy to the rare earth ions. For increasing annealing temperatures, this 920 nm-emission decreases. It has been ascribed to both the formation of Nd_2O_3 clusters and the increasing sensitizer: Nd^{3+} distance. As studied on the mechanism of excitation towards Nd^{3+} ions, two kinds of sensitizers (radiative defects and atomic scale entities) would coexist for low T_A -annealed Nd-SiO_x films, while Si-ncs were grown acting as sensitizer for high T_A films. This would allow one to obtain high content of Nd^{3+} ions sensitized, which is the key parameter to achieve future photonic component.

ACKNOWLEDGMENTS

The authors thank the French National Agency (ANR) and Chinese Scholarship Council (CSC), which supported this work through the Nanoscience and Nanotechnology Program (DAPHNES Project ANR-08-NANO-005).

- ¹L. Khriachtchev, *Silicon Nanophotonics: Basic Principles, Present Status and Perspectives* (Pan Stanford Publishing, Singapore, 2008), Chap. 1.
- ²L. Pavesi and R. Turan, *Silicon Nanocrystals: Fundamentals, Synthesis and Applications* (Wiley, New York, 2010), Chap. 2.
- ³J. P. Proot, C. Delerue, and G. Allan, *Appl. Phys. Lett.* **61**, 1948 (1992).
- ⁴T. Inokuma, Y. Wakayama, T. Muramoto, R. Aoki, Y. Kurata, and S. Hasegawa, *J. Appl. Phys.* **83**, 2228 (1998).
- ⁵F. Iacona, G. Franzò, and C. Spinella, *J. Appl. Phys.* **87**, 1295 (2000).
- ⁶C. Dufour, S. Chausserie, and F. Gourbilleau, *J. Lumin.* **129**, 73 (2009).
- ⁷A. J. Kenyon, P. F. Trwoga, M. Federighi, and C. W. Pitt, *J. Phys.:Condens. Matter* **6**, L319 (1994).
- ⁸A. J. Kenyon, C. E. Chryssou, C. W. Pitt, T. Shimizu-Iwayama, D. E. Hole, N. Sharma, and C. J. Humphreys, *J. Appl. Phys.* **91**, 367 (2002).
- ⁹I. Izeddin, A. S. Moskalenko, I. N. Yassievich, M. Fujii, and T. Gregorkiewicz, *Phys. Rev. Lett.* **97**, 207401 (2006).
- ¹⁰A. Pitanti, D. Navarro-Urrios, N. Prtljaga, N. Daldosso, F. Gourbilleau, R. Rizk, B. Garrido, and L. Pavesi, *J. Appl. Phys.* **108**, 053518 (2010).
- ¹¹J. M. Ramírez, F. F. Lupi, O. Jambois, Y. Berencén, D. Navarro-Urrios, A. Anopchenko, A. Marconi, N. Prtljaga, A. Tengattini, L. Pavesi, J. P. Colonna, J. M. Fedeli, and B. Garrido, *Nanotechnology* **23**, 125203 (2012).
- ¹²O. Savchyn, R. M. Todi, K. R. Coffey, and P. G. Kik, *Appl. Phys. Lett.* **93**, 233120 (2008).
- ¹³A. N. MacDonald, A. Hryciw, F. Lenz, and A. Meldrum, *Appl. Phys. Lett.* **89**, 173132 (2006).
- ¹⁴J. S. Chang, J. H. Jhe, M. S. Yang, J. H. Shin, K. J. Kim, and D. W. Moon, *Appl. Phys. Lett.* **89**, 181909 (2006).
- ¹⁵F. Priolo, G. Franzò, D. Pacifici, V. Vinciguerra, F. Iacona, and A. Irrera, *J. Appl. Phys.* **89**, 264 (2001).
- ¹⁶J. H. Jhe, J. H. Shin, K. J. Kim, and D. W. Moon, *Appl. Phys. Lett.* **82**, 4489 (2003).
- ¹⁷M. Fujii, K. Imakita, K. Watanabe, and S. Hayashi, *J. Appl. Phys.* **95**, 272 (2004).
- ¹⁸H. S. Han, S. Y. Seo, and J. H. Shin, *Appl. Phys. Lett.* **79**, 4568 (2001).
- ¹⁹S. L. Oliveira, D. F. de Sousa, A. A. Andrade, L. A. O. Nunes, and T. Catunda, *J. Appl. Phys.* **103**, 023103 (2008).
- ²⁰D. Navarro-Urrios, A. Pitanti, N. Daldosso, F. Gourbilleau, L. Khomenkova, R. Rizk, and L. Pavesi, *Physica E* **41**, 1029 (2009).
- ²¹S. Y. Seo, M.-J. Kim, and J. H. Shin, *Appl. Phys. Lett.* **83**, 2778 (2003).
- ²²E. Steveler, H. Rinnert, and M. Vergnat, *J. Appl. Phys.* **110**, 113518 (2011).
- ²³A. Podhorodecki, J. Misiewicz, F. Gourbilleau, J. Cardin, and C. Dufour, *Electrochem. Solid State* **13**, K26 (2010).
- ²⁴O. Debieu, D. Bréard, A. Podhorodecki, G. Zatoryb, J. Misiewicz, C. Labbé, J. Cardin, and F. Gourbilleau, *J. Appl. Phys.* **108**, 113114 (2010).
- ²⁵K. Watanabe, H. Tamaoka, M. Fujii, K. Moriwaki, and S. Hayashi, *Physica E* **13**, 1038 (2002).
- ²⁶N. M. Park, C. J. Choi, T. Y. Seong, and S. J. Park, *Phys. Rev. Lett.* **86**, 1355 (2001).
- ²⁷A. Podhorodecki, G. Zatoryb, J. Misiewicz, J. Wojcik, and P. Mascher, *J. Appl. Phys.* **102**, 043104 (2007).
- ²⁸F. Koch, V. Petrova-Koch, and T. Muschik, *J. Lumin.* **57**, 271 (1993).
- ²⁹S. M. Prokes, *Appl. Phys. Lett.* **62**, 3244 (1993).
- ³⁰M. Wang, D. Yang, D. Li, Z. Yuan, and D. Que, *J. Appl. Phys.* **101**, 103504 (2007).
- ³¹D. Bréard, F. Gourbilleau, A. Belarouci, C. Dufour, and R. Rizk, *J. Lumin.* **121**, 209 (2006).
- ³²C.-H. Liang, O. Debieu, Y.-T. An, L. Khomenkova, J. Cardin, and F. Gourbilleau, *J. Lumin.* **132**, 3118 (2012).
- ³³G. Wora Adeola, H. Rinnert, P. Miska, and M. Vergnat, *J. Appl. Phys.* **102**, 053515 (2007).
- ³⁴B. Garrido Fernandez, M. Lopez, C. Garcia, A. Perez-Rodriguez, J. R. Morante, C. Bonafos, M. Carrada, and A. Claverie, *J. Appl. Phys.* **91**, 798 (2002).

- ³⁵M. Roussel, E. Talbot, P. Pareige, and F. Gourbilleau, *J. Appl. Phys.* **113**, 063519 (2013).
- ³⁶C. H. Liang, J. Cardin, L. Khomenkova, and F. Gourbilleau, *Proc. SPIE* **8431**, 84311Y (2012).
- ³⁷J. E. Olsen and F. Shimura, *J. Appl. Phys.* **66**, 1353 (1989).
- ³⁸E. Talbot, R. Larde, P. Pareige, L. Khomenkova, K. Hijazi, and F. Gourbilleau, *Nanoscale Res. Lett.* **8**, 39 (2013).
- ³⁹O. Savchyn, F. R. Ruhge, P. G. Kik, R. M. Todi, K. R. Coffey, H. Nukala, and H. Heinrich, *Phys. Rev. B* **76**, 195419 (2007).
- ⁴⁰Y. H. Xie, M. S. Hybertsen, W. L. Wilson, S. A. Ipri, G. E. Carver, W. L. Brown, E. Dons, B. E. Weir, A. R. Kortan, G. P. Watson, and A. J. Liddle, *Phys. Rev. B* **49**, 5386 (1994).
- ⁴¹L. N. Dinh, L. L. Chase, M. Balooch, W. J. Siekhaus, and F. Wooten, *Phys. Rev. B* **54**, 5029 (1996).
- ⁴²M. L. Brongersma, A. Polman, K. S. Min, E. Boer, T. Tambo, and H. A. Atwater, *Appl. Phys. Lett.* **72**, 2577 (1998).
- ⁴³B. Garrido, C. García, S. Y. Seo, P. Pellegrino, D. Navarro-Urrios, N. Daldosso, L. Pavesi, F. Gourbilleau, and R. Rizk, *Phys. Rev. B* **76**, 245308 (2007).
- ⁴⁴D. Pacifici, G. Franzò, F. Priolo, F. Iacona, and L. Dal Negro, *Phys. Rev. B* **67**, 245301 (2003).
- ⁴⁵P. Vergeer, T. J. H. Vlugt, M. H. F. Kox, M. I. den Hertog, J. P. J. M. van der Eerden, and A. Meijerink, *Phys. Rev. B* **71**, 014119 (2005).
- ⁴⁶R. Li, S. Yerci, S. O. Kucheyev, T. van Buuren, and L. Dal Negro, *Opt. Express* **19**, 5379 (2011).
- ⁴⁷F. Gourbilleau, M. Levalois, C. Dufour, J. Vicens, and R. Rizk, *J. Appl. Phys.* **95**, 3717 (2004).
- ⁴⁸P. Horak, W. H. Loh, and A. J. Kenyon, *Opt. Express* **17**, 906 (2009).